

# RSC Advances



This is an *Accepted Manuscript*, which has been through the Royal Society of Chemistry peer review process and has been accepted for publication.

*Accepted Manuscripts* are published online shortly after acceptance, before technical editing, formatting and proof reading. Using this free service, authors can make their results available to the community, in citable form, before we publish the edited article. This *Accepted Manuscript* will be replaced by the edited, formatted and paginated article as soon as this is available.

You can find more information about *Accepted Manuscripts* in the [Information for Authors](#).

Please note that technical editing may introduce minor changes to the text and/or graphics, which may alter content. The journal's standard [Terms & Conditions](#) and the [Ethical guidelines](#) still apply. In no event shall the Royal Society of Chemistry be held responsible for any errors or omissions in this *Accepted Manuscript* or any consequences arising from the use of any information it contains.

## COMMUNICATION

## Z-scheme photocatalytic hydrogen production over WO<sub>3</sub>/g-C<sub>3</sub>N<sub>4</sub> composite photocatalysts<sup>†</sup>

Cite this: DOI: 10.1039/x0xx00000x

Hideyuki Katsumata,<sup>\*a</sup> Yusuke Tachi,<sup>a</sup> Tohru Suzuki<sup>b</sup> and Satoshi Kaneco<sup>a</sup>Received 00th January 2012,  
Accepted 00th January 2012

DOI: 10.1039/x0xx00000x

www.rsc.org/

**WO<sub>3</sub>/g-C<sub>3</sub>N<sub>4</sub> composite photocatalysts were prepared by a simple calcination method and H<sub>2</sub> production activity of these composites was evaluated. The photocatalytic activity of the composites highly depended on WO<sub>3</sub> content. The enhanced photocatalytic activity could be ascribed to the Z-scheme mechanism, which results in the efficient charge separation.**

As a typical metal free inorganic semiconductor, graphitic C<sub>3</sub>N<sub>4</sub> (g-C<sub>3</sub>N<sub>4</sub>) has attracted intensive attention for H<sub>2</sub> generation,<sup>1</sup> pollutant degradation<sup>2</sup> and CO<sub>2</sub> reduction.<sup>3</sup> It is well-known that the band gap of g-C<sub>3</sub>N<sub>4</sub> is about 2.7 eV, which can absorb visible light up to 460 nm.<sup>4</sup> Furthermore, the CB minimum (−1.12 eV vs. NHE) of g-C<sub>3</sub>N<sub>4</sub> is extremely negative, so photo-generated electrons should have high reduction ability. However, the photocatalytic efficiency of the pure g-C<sub>3</sub>N<sub>4</sub> is limited by the high recombination rate of its photo-generated electron–hole pairs.<sup>5</sup> One of the techniques for increasing the separation efficiency of photo-generated electron–hole pairs is to form a composite photocatalyst using two kinds of semiconductors. Suitable matching of the band levels of the conduction and valence bands in the two semiconductors offers appropriate driving forces to separate and transfer photo-generated electron–hole pairs.<sup>6</sup> To improve g-C<sub>3</sub>N<sub>4</sub> photocatalytic activity, various semiconductor/g-C<sub>3</sub>N<sub>4</sub> composite photocatalysts have been reported, such as ZnO,<sup>7</sup> TiO<sub>2</sub>,<sup>8</sup> Ag<sub>3</sub>PO<sub>4</sub>,<sup>9</sup> AgBr,<sup>10</sup> Bi<sub>2</sub>WO<sub>6</sub>,<sup>11</sup> MoS<sub>2</sub>,<sup>12</sup>, etc, and used for the photodegradation of organic dyes in solution. However, the photocatalytic H<sub>2</sub> production over semiconductor/g-C<sub>3</sub>N<sub>4</sub> composite photocatalysts has been proposed in limited reports.<sup>13</sup>

On the other hand, studies have shown that WO<sub>3</sub> is a visible-light responsive photocatalyst with a relatively narrow band-gap energy (2.4–2.8 eV) and a VB potential similar to that of TiO<sub>2</sub>.<sup>14</sup> Therefore, the oxidizing power of holes in the VB of WO<sub>3</sub> and TiO<sub>2</sub> are considered to be almost the same. However, pure WO<sub>3</sub> is not an efficient photocatalyst because of its low CB level, which limits the photocatalyst's ability to react with electron acceptors such as oxygen.<sup>15</sup> The low CB level also increases the recombination of photo-generated electron–hole pairs leading to lower photocatalytic activity. Many attempts

have been made to improve the photocatalytic activity of WO<sub>3</sub>, such as noble metal loading<sup>16</sup> and coupling with other semiconductors.<sup>17</sup> In our previous study, The activity of WO<sub>3</sub> particles could be significantly improved by the binary loading of Ag and CuO as cocatalysts.<sup>18</sup> Among them, studies have confirmed that WO<sub>3</sub> is a good candidate for synthesizing semiconductor heterojunctions with higher photocatalytic activity. As WO<sub>3</sub> and g-C<sub>3</sub>N<sub>4</sub> are both visible-light-driven photocatalysts, after the polymeric g-C<sub>3</sub>N<sub>4</sub> photocatalyst being combined with WO<sub>3</sub> the obtained WO<sub>3</sub>/g-C<sub>3</sub>N<sub>4</sub> composite may be a promising candidate for efficient photocatalytic activity under solar light irradiation. However, there are a few reports on the photocatalytic activity evaluation of WO<sub>3</sub>/g-C<sub>3</sub>N<sub>4</sub> composite.<sup>19,20</sup> Furthermore, to the best of our knowledge, there are no reports on the application of WO<sub>3</sub>/g-C<sub>3</sub>N<sub>4</sub> composite photocatalysts for H<sub>2</sub> production from aqueous solution, and no attention has been paid to the photocatalytic mechanism of the composite-catalysed reaction, which has remained unclear to date.

In this paper, different ratios of WO<sub>3</sub>/g-C<sub>3</sub>N<sub>4</sub> composite photocatalysts were synthesized via the calcination process. The photocatalysts were characterized by various techniques such as powder X-ray diffraction (XRD), scanning electron microscopy (SEM), transmission electron microscopy (TEM), UV-visible diffuse reflectance spectra (DRS), and so on. The photocatalytic activity was evaluated by H<sub>2</sub> production from triethanolamine (TEA) aqueous solution under artificial solar light. The separation mechanisms of photo-excited carriers for the composite photocatalysts were also proposed on the basis of the results for the photoluminescence (PL) analysis.

The XRD patterns of WO<sub>3</sub>/g-C<sub>3</sub>N<sub>4</sub> composites, g-C<sub>3</sub>N<sub>4</sub> and WO<sub>3</sub> are shown in Fig. 1. For pure g-C<sub>3</sub>N<sub>4</sub>, two broad diffraction peaks around 27.5 and 13.0° were observed, corresponding to the (002) and (100) diffraction planes, respectively. The former, which corresponds to the interlayer distance of 0.325 nm, is attributed to the long-range interplanar stacking of aromatic units; the latter with a much weaker intensity, which corresponds to a distance *d* = 0.681 nm, is associated with interlayer stacking.<sup>1</sup> For WO<sub>3</sub>/g-C<sub>3</sub>N<sub>4</sub> composites, the XRD patterns reveal a coexistence of WO<sub>3</sub> and g-C<sub>3</sub>N<sub>4</sub>. The peak intensities of g-C<sub>3</sub>N<sub>4</sub> rapidly decreased with increasing the WO<sub>3</sub> contents. It is difficult to confirm the diffraction

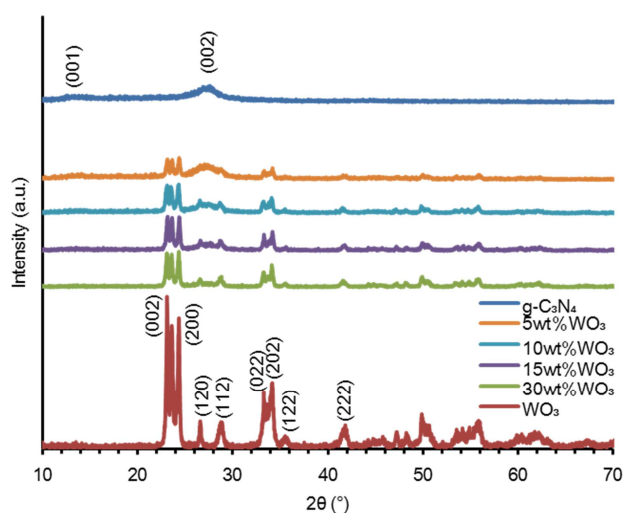


Fig. 1. XRD patterns of g-C<sub>3</sub>N<sub>4</sub>, WO<sub>3</sub> and WO<sub>3</sub>/g-C<sub>3</sub>N<sub>4</sub> composite photocatalyst.

peaks of g-C<sub>3</sub>N<sub>4</sub> in the XRD pattern of the 30 wt% WO<sub>3</sub>/g-C<sub>3</sub>N<sub>4</sub> sample. The XRD pattern of WO<sub>3</sub> could be indexed as the monoclinic structure. These results along with FTIR spectra (Fig. S1) and XPS spectra (Fig. S2) showed clearly that WO<sub>3</sub>/g-C<sub>3</sub>N<sub>4</sub> composite photocatalysts could be synthesized by the calcination method.

Fig. 2 shows SEM and TEM images of g-C<sub>3</sub>N<sub>4</sub>, WO<sub>3</sub> and 10 wt% WO<sub>3</sub>/g-C<sub>3</sub>N<sub>4</sub> composite samples. It is clearly seen in Fig. 2a and d that the morphology of g-C<sub>3</sub>N<sub>4</sub> was smooth, thin and flat sheets. In addition, a typical porous morphology of g-C<sub>3</sub>N<sub>4</sub> powders was exhibited.<sup>21</sup> From Fig. 2b and e, WO<sub>3</sub> showed aggregated particles with the particle size of 20–150 nm. In the composite sample, WO<sub>3</sub> particles were sparsely observed onto the g-C<sub>3</sub>N<sub>4</sub> surface. WO<sub>3</sub> particles did not agglomerate and were directly attached to the surface of g-C<sub>3</sub>N<sub>4</sub>. With increasing WO<sub>3</sub> content, a

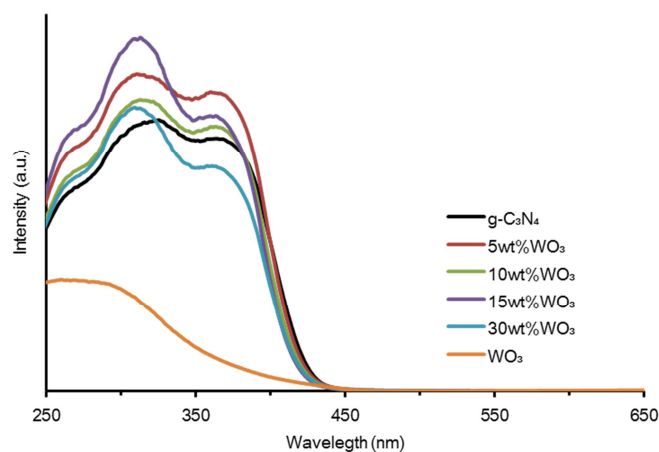


Fig. 3. UV-vis DRS of g-C<sub>3</sub>N<sub>4</sub>, WO<sub>3</sub> and WO<sub>3</sub>/g-C<sub>3</sub>N<sub>4</sub> composite photocatalyst.

large number of WO<sub>3</sub> particles were observed on the g-C<sub>3</sub>N<sub>4</sub> surface (Fig. S3a-c). Further, HRTEM observation was conducted to investigate the interfacial structure of the composite sample (Fig. S3d). The (020) lattice fringe of monoclinic WO<sub>3</sub> (0.375 nm) was clearly observed in the HRTEM image. The gray area can be ascribed to g-C<sub>3</sub>N<sub>4</sub>. From the SEM, TEM and HRTEM analyses, it can be concluded that the heterojunction structure was formed in the composite.

The UV-vis DRS of g-C<sub>3</sub>N<sub>4</sub>, WO<sub>3</sub> and all composite photocatalysts are shown in Fig. 3. For all samples, the optical absorption edge was estimated to be at around 450 nm. The composite samples displayed better photon absorption than both WO<sub>3</sub> and g-C<sub>3</sub>N<sub>4</sub> because the composites would have high crystallinity due to the calcination at 450°C during the composite photocatalysts preparation. The band gap can be estimated from the following equation:

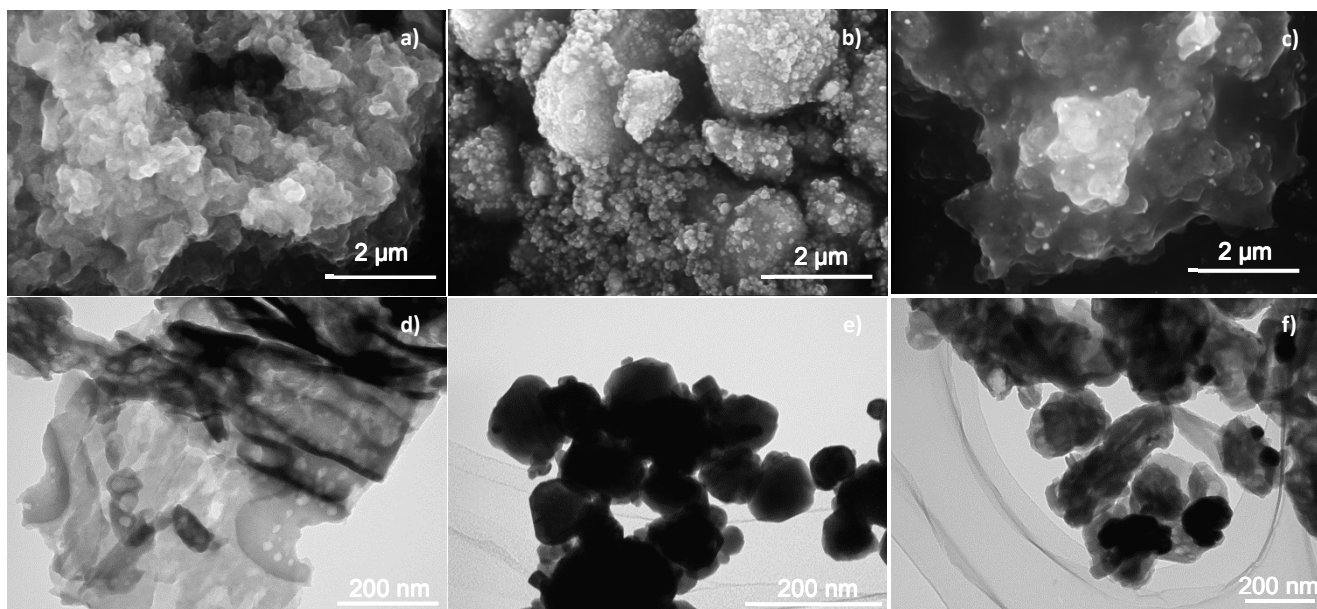


Fig. 2. SEM and TEM images of (a), (d) g-C<sub>3</sub>N<sub>4</sub>; (b), (e) WO<sub>3</sub>; (c), (f) 10 wt% WO<sub>3</sub>/g-C<sub>3</sub>N<sub>4</sub>.

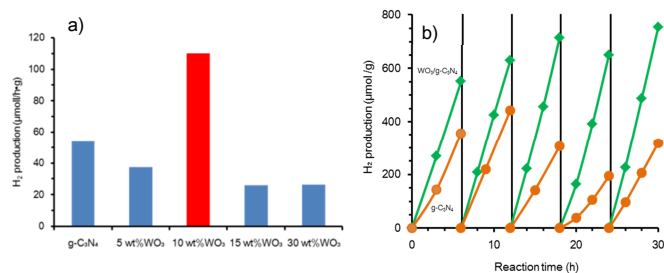


Fig. 4. (a) Photocatalytic H<sub>2</sub> production over g-C<sub>3</sub>N<sub>4</sub> and WO<sub>3</sub>/g-C<sub>3</sub>N<sub>4</sub> composite photocatalysts under artificial solar light irradiation; (b) Time courses of H<sub>2</sub> production over g-C<sub>3</sub>N<sub>4</sub> and 10 wt% WO<sub>3</sub>/g-C<sub>3</sub>N<sub>4</sub> composite photocatalyst artificial solar light irradiation.

$$ah\nu = A(h\nu - E_g)^{n/2}$$

where  $a$ ,  $h$ ,  $\nu$ , and  $E_g$  are the absorption coefficient, Planck's constant, light frequency, and band gap, respectively, and  $A$  is a constant. The factor  $n$  depends on the characteristics of the optical transition of a semiconductor ( $n = 1$  for direct transition and  $n = 4$  for indirect transition). The band gaps of g-C<sub>3</sub>N<sub>4</sub> and WO<sub>3</sub> were estimated to be 2.78 and 2.60 eV, respectively (Fig. S4).<sup>1,14</sup> After coupling these two semiconductors, the band gaps of WO<sub>3</sub>/g-C<sub>3</sub>N<sub>4</sub> composite photocatalysts kept at around 2.8 eV, implying the composite photocatalysts are also responsible for the visible light region.

The photocatalytic H<sub>2</sub> production over the all samples is shown in Fig. 4a. It revealed that the loading of WO<sub>3</sub> greatly influenced the photocatalytic performance of g-C<sub>3</sub>N<sub>4</sub>. The H<sub>2</sub> production rate over g-C<sub>3</sub>N<sub>4</sub> was 54  $\mu\text{mol h}^{-1} \text{g}^{-1}$ . As a comparison, the composite photocatalysts showed that the H<sub>2</sub> production rates were lower than that on g-C<sub>3</sub>N<sub>4</sub> except for 10 wt% WO<sub>3</sub>/g-C<sub>3</sub>N<sub>4</sub> photocatalyst in which the H<sub>2</sub> production rate was 110  $\mu\text{mol h}^{-1} \text{g}^{-1}$ , i.e., the photocatalytic activity of this composite was about 2 times higher than that of g-C<sub>3</sub>N<sub>4</sub>. However, the photocatalytic activity of the mechanical mixture of WO<sub>3</sub> and g-C<sub>3</sub>N<sub>4</sub> sample with 10 wt% WO<sub>3</sub> content (60  $\mu\text{mol h}^{-1} \text{g}^{-1}$ ) was almost the same as that of pure g-C<sub>3</sub>N<sub>4</sub>. The photocatalytic activity of 10 wt% WO<sub>3</sub>/g-C<sub>3</sub>N<sub>4</sub> composite was also evaluated under visible light irradiation (>420 nm). As a result, the H<sub>2</sub> production rate over 10 wt% WO<sub>3</sub>/g-C<sub>3</sub>N<sub>4</sub> (66  $\mu\text{mol h}^{-1} \text{g}^{-1}$ )

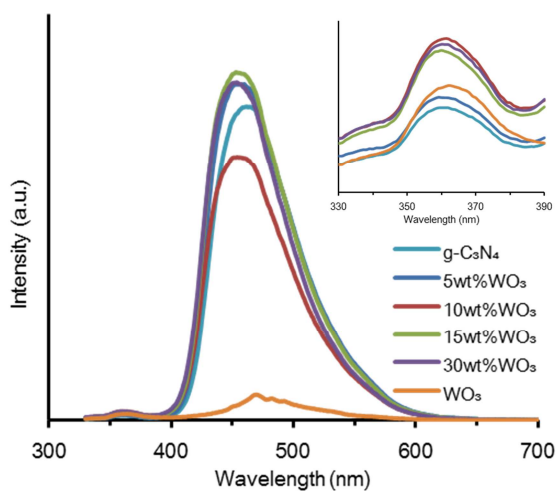


Fig. 5. PL spectra of g-C<sub>3</sub>N<sub>4</sub>, WO<sub>3</sub> and WO<sub>3</sub>/g-C<sub>3</sub>N<sub>4</sub> composite photocatalysts.

was higher than that of g-C<sub>3</sub>N<sub>4</sub> (27  $\mu\text{mol h}^{-1} \text{g}^{-1}$ ) under visible light irradiation. The apparent quantum efficiencies at 405 nm were 0.34 and 0.90% for g-C<sub>3</sub>N<sub>4</sub> and 10 wt% WO<sub>3</sub>/g-C<sub>3</sub>N<sub>4</sub>, respectively.

Fig. 4b shows the time courses of H<sub>2</sub> production obtained over g-C<sub>3</sub>N<sub>4</sub> and 10 wt% WO<sub>3</sub>/g-C<sub>3</sub>N<sub>4</sub> samples under light irradiation. For both samples, the production of H<sub>2</sub> steadily increased with prolonged time of light irradiation. However, the photocatalytic activity of g-C<sub>3</sub>N<sub>4</sub> for H<sub>2</sub> production gradually decreased during the photocatalytic reaction and a total H<sub>2</sub> production was about 1.6 mmol g<sup>-1</sup> (36 mL g<sup>-1</sup>) after 30 h. On the other hand, a total of 3.3 mmol g<sup>-1</sup> H<sub>2</sub> gas (74 mL g<sup>-1</sup>) was produced over 10 wt% WO<sub>3</sub>/g-C<sub>3</sub>N<sub>4</sub>, and no obvious deactivation of the composite photocatalyst was found, suggesting the good stability of WO<sub>3</sub>/g-C<sub>3</sub>N<sub>4</sub> as an organic-inorganic composite photocatalyst for solar H<sub>2</sub> production. Furthermore, no changes of the composite sample after photocatalytic reaction were observed in XRD pattern and TEM image (Fig. S5).

To understand the higher photocatalytic activity of 10 wt% WO<sub>3</sub>/g-C<sub>3</sub>N<sub>4</sub> relative to other composites, g-C<sub>3</sub>N<sub>4</sub> and WO<sub>3</sub>, the PL spectra of the samples at 270 nm were recorded (Fig. 5). It is clear that the PL spectra of the composite and g-C<sub>3</sub>N<sub>4</sub> photocatalysts have a strong emission peak at around 450 nm, which could be related to the recombination of the photo-excited electron-hole of g-C<sub>3</sub>N<sub>4</sub>.<sup>7,11,22</sup> While a weak emission peak at around 460 nm of WO<sub>3</sub> was assigned to localized state in the band gap due to oxygen vacancies or defects.<sup>23</sup> From Fig. 5, it can be seen that the PL intensities of the 5, 15 and 30 wt% WO<sub>3</sub>/g-C<sub>3</sub>N<sub>4</sub> photocatalysts exhibited the stronger emission than that of the pure g-C<sub>3</sub>N<sub>4</sub>, suggesting that the recombination of the photo-excited electron-hole on the g-C<sub>3</sub>N<sub>4</sub> photocatalyst surface is higher. On the contrary, the PL intensity of 10 wt% WO<sub>3</sub>/g-C<sub>3</sub>N<sub>4</sub> composite photocatalyst was lower than that of pure g-C<sub>3</sub>N<sub>4</sub>, which means that the recombination of the photo-excited electron-hole of the composite photocatalyst was lower than pure g-C<sub>3</sub>N<sub>4</sub>. It indicates that when the amount of WO<sub>3</sub> is suitable (10 wt%), the recombination of the photo-excited electron-hole on the g-C<sub>3</sub>N<sub>4</sub> surface is suppressed. However, 10 wt% WO<sub>3</sub>/g-C<sub>3</sub>N<sub>4</sub> showed the highest PL intensity at around 360 nm among the all samples examined (inset of Fig. 5). The peak around at 360 nm was assigned to the electron-hole recombination on the WO<sub>3</sub> surface.<sup>23</sup> Therefore, the recombination of the charge carriers on the interface of 10 wt% WO<sub>3</sub>/g-C<sub>3</sub>N<sub>4</sub> in the composite photocatalyst would be higher than that of pure WO<sub>3</sub>. The PL results are agreement with the results of photocatalytic H<sub>2</sub> production onto WO<sub>3</sub>/g-C<sub>3</sub>N<sub>4</sub> composite photocatalysts. It means that higher and lower PL intensities at 360

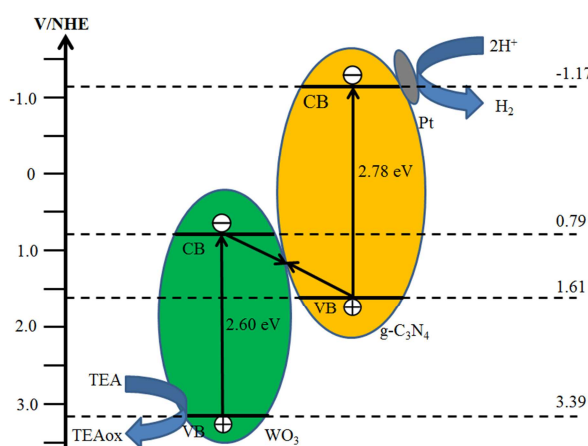


Fig. 6. Schematic diagram of Z-scheme photocatalytic mechanism of WO<sub>3</sub>/g-C<sub>3</sub>N<sub>4</sub> composite photocatalyst.

and 450 nm indicate a higher photocatalytic activity in the experimental conditions. The higher PL intensities at 360 nm of the samples would be attributed to the higher recombination rate between photo-excited electrons in the CB of WO<sub>3</sub> and photo-excited holes in the VB of g-C<sub>3</sub>N<sub>4</sub> on the interface of the composite, suggesting that rich electrons in the CB of g-C<sub>3</sub>N<sub>4</sub> and holes in the VB of WO<sub>3</sub> participate in the reduction reaction of H<sup>+</sup> and the oxidation of TEA, respectively. As a result, the charge separation could be promoted on the 10 wt% WO<sub>3</sub>/g-C<sub>3</sub>N<sub>4</sub> composite, leading to the higher photocatalytic activity of the composite photocatalyst. Based on these results, it could be concluded that the WO<sub>3</sub>/g-C<sub>3</sub>N<sub>4</sub> system is a typical Z-scheme photocatalyst.

On the basis of the above results, the photocatalytic mechanism for the WO<sub>3</sub>/g-C<sub>3</sub>N<sub>4</sub> composite sample is tentatively proposed and schematically illustrated in Fig. 6. For pure g-C<sub>3</sub>N<sub>4</sub>, the photo-generated electrons and holes in g-C<sub>3</sub>N<sub>4</sub> tend to recombine and only a fraction of them participates in the photocatalytic reaction, resulting in a relative low activity. For WO<sub>3</sub>/g-C<sub>3</sub>N<sub>4</sub> composite with an optimal WO<sub>3</sub> content, i.e. 10 wt%, part of the surface of g-C<sub>3</sub>N<sub>4</sub> is covered by WO<sub>3</sub> particles, leading to the formation of Z-scheme photocatalytic system. According to previous studies, the CB and VB positions of WO<sub>3</sub> are about +0.74 and +3.4 V, respectively,<sup>15</sup> while those of g-C<sub>3</sub>N<sub>4</sub> are about -1.13 and +1.57 V, respectively.<sup>22</sup> Further, the band structure of WO<sub>3</sub>/g-C<sub>3</sub>N<sub>4</sub> used in this study can be also estimated according to the empirical equations as shown below:

$$E_{\text{VB}} = \chi - E^e + 0.5E_g$$

$$E_{\text{CB}} = E_{\text{VB}} - E_g$$

where  $E_{\text{VB}}$  and  $E_{\text{CB}}$  are the valence and conduction band edge potentials, respectively;  $\chi$  is the electronegativity of the semiconductor, which is the geometric mean of the electronegativity of the constituent atoms;  $E^e$  is the energy of free electrons on the hydrogen scale (about 4.5 eV vs. NHE). The estimated CB and VB positions for WO<sub>3</sub> and g-C<sub>3</sub>N<sub>4</sub> are shown in Fig. 6 and were similar values to those of previous studies.<sup>15,22</sup> Thus, under artificial solar light irradiation, the photo-induced holes tend to keep in the VB of WO<sub>3</sub>, while the electrons in CB of WO<sub>3</sub> combine with the holes in VB of g-C<sub>3</sub>N<sub>4</sub> at the interface of the composite. The electrons in the VB of g-C<sub>3</sub>N<sub>4</sub> are further excited to its CB. This results in an efficient space separation of the photo-induced charge carriers. Then, the electrons stored in the CB of g-C<sub>3</sub>N<sub>4</sub> react with H<sup>+</sup> in water near the surface of the photocatalyst to produce H<sub>2</sub> gas while the holes in the VB of WO<sub>3</sub> oxidize TEA molecules. The above hydrogen production experiments and PL analysis would support the Z-scheme photocatalytic mechanism. If the charge carriers of WO<sub>3</sub>/g-C<sub>3</sub>N<sub>4</sub> photocatalyst transfer according to the conventional electron-hole separation process for a great number of composite photocatalysts; the electrons in the CB of g-C<sub>3</sub>N<sub>4</sub> would migrate to the CB of WO<sub>3</sub>, and holes in the VB of WO<sub>3</sub> would transfer to the VB of g-C<sub>3</sub>N<sub>4</sub>. This can result from the efficient charge separation of the photo-induced charge carriers. However, the electrons in the CB of WO<sub>3</sub> cannot produce H<sub>2</sub> gas from water because the CB potential of WO<sub>3</sub> is positive than that of the H<sub>2</sub>/H<sup>+</sup> couple. In addition, the oxidation power of the composite photocatalyst decreases because the VB potential of g-C<sub>3</sub>N<sub>4</sub> is relatively low. This would lead that the WO<sub>3</sub>/g-C<sub>3</sub>N<sub>4</sub> composite has a lower reduction/oxidation ability and photocatalytic activity than pure g-C<sub>3</sub>N<sub>4</sub> and WO<sub>3</sub>. Therefore, it can be concluded that the photocatalytic mechanism of WO<sub>3</sub>/g-C<sub>3</sub>N<sub>4</sub> composite is not accordance with the traditional charge separation process.

Namely, a typical Z-scheme photocatalyst is favourable for the production of H<sub>2</sub> gas from water. The Z-scheme mechanism of WO<sub>3</sub>/g-C<sub>3</sub>N<sub>4</sub> composite photocatalyst has been also reported by the other researchers.<sup>20</sup>

In this study, the unsuitable contents of WO<sub>3</sub> in WO<sub>3</sub>/g-C<sub>3</sub>N<sub>4</sub> photocatalyst showed low photocatalytic activity for H<sub>2</sub> production. Unfortunately, the reasons are not fully understood currently. We need the further studies to be clear the more detail photocatalytic mechanism of WO<sub>3</sub>/g-C<sub>3</sub>N<sub>4</sub> composite.

## Conclusions

In summary, the composite photocatalyst WO<sub>3</sub>/g-C<sub>3</sub>N<sub>4</sub> was fabricated via a simple calcination method. The highest photocatalytic activity was achieved for 10 wt% WO<sub>3</sub>/g-C<sub>3</sub>N<sub>4</sub> composite at H<sub>2</sub> production rate of 110 μmol h<sup>-1</sup> g<sup>-1</sup>, which was about 2 times higher compared to that of pure g-C<sub>3</sub>N<sub>4</sub>. Furthermore, the composite showed a good stability for the repeated H<sub>2</sub> production reaction. The enhanced activity was due to the formation of WO<sub>3</sub>/g-C<sub>3</sub>N<sub>4</sub> Z-scheme photocatalytic system and an efficient charge separation of the photo-generated electron-hole pairs. This present study would provide new insights on enhancing the photocatalytic H<sub>2</sub> production activity of g-C<sub>3</sub>N<sub>4</sub> by the formation of Z-scheme WO<sub>3</sub>/g-C<sub>3</sub>N<sub>4</sub> composite photocatalyst.

## Acknowledgements

This work was partly supported by Grant-in-Aid for Scientific Research (C) No. 24510095 from the Ministry of Education, Culture, Sports, Science, and Technology of Japan.

## Notes and references

<sup>a</sup> Department of Chemistry for Materials, Graduate School of Engineering, Mie University, Tsu, Mie 514-8507, Japan. E-mail: hidek@chem.mie-u.ac.jp; Fax: +81-59231-9425; Tel: +81-59231-9425

<sup>b</sup> Environmental Preservation Center, Mie University, Tsu, Mie 514-8507, Japan.

† Electronic Supplementary Information (ESI) available: [Experimental details and Figs. S1-S5]. See DOI: 10.1039/c000000x/

- X. C. Wang, K. Maeda, A. Thomas, K. Takanabe, G. Xin, J. M. Carlsson, K. Domen and M. Antonietti, *Nat. Mater.*, 2009, **8**, 76; Q. J. Xiang, J. G. Yu and M. Jaroniec, *J. Phys. Chem. C*, 2011, **115**, 7355; J. G. Yu, S. H. Wang, B. Cheng, Z. Lin and F. Huang, *Catal. Sci. Technol.*, 2013, **3**, 1782.
- Y. J. Cui, Z. X. Ding and X. Z. Fu, *Angew. Chem., Int. Ed.*, 2012, **51**, 11814.
- G. H. Dong and L. Z. Zhang, *J. Mater. Chem.*, 2012, **22**, 1160; J. Mao, T. Peng, X. Zhang, K. Li, L. Ye and L. Zan, *Catal. Sci. Technol.*, 2013, **3**, 1253.
- X. Wang, K. Maeda, X. Chen, K. Takanabe, K. Domen, Y. Hou, X. Fu and M. Antonietti, *J. Am. Chem. Soc.*, 2009, **131**, 1680; Y. Wang, X. Wang and M. Antonietti, *Angew. Chem., Int. Ed.*, 2012, **51**, 68.
- S. C. Yan, Z. S. Li and Z. G. Zou, *Langmuir*, 2009, **25**, 10397.
- J. Zhang, M. Zhang, R. Q. Sun and X. Wang, *Angew. Chem., Int. Ed.*, 2012, **51**, 10145.

- 7 Y. J. Wang, R. Shi, J. Lin and Y. F. Zhu, *Energy Environ. Sci.*, 2011, **4**, 2922; J.X. Sun, Y.P. Yuan, L.G. Qiu, X. Jiang, A.J. Xie, Y.H. Shen and J.F. Zhu, *Dalton Trans.*, 2012, **41**, 6756.
- 8 X. Lu, Q. Wang and D. Cui, *J. Mater. Sci. Technol.*, 2010, **26**, 925.
- 9 S. Kumar, T. Surendar, A. Baruah and V. Shanker, *J. Mater. Chem. A*, 2013, **1**, 5333.
- 10 H. Xu, J. Yan, Y. G. Xu, Y. H. Song, H. M. Li, J. X. Xia, C. J. Huang and H. L. Wan, *Appl. Catal. B*, 2013, **129**, 182; S. Yang, W. Zhou, C. Ge, X. Liu, Y. Fang and Z. Li, *RSC Adv.*, 2013, **3**, 5631.
- 11 L. Ge, C. Han and J. Liu, *Appl. Catal. B*, 2011, **108/109**, 100.
- 12 W. C. Peng and X. Y. Li, *Catal. Commun.*, 2014, **49**, 63.
- 13 B. Chai, T. Peng, J. Mao, K. Li and L. Zan, *Phys. Chem. Chem. Phys.*, 2012, **14**, 16745; Y. D. Hou, A. B. Laursen, J. S. Zhang, G. G. Zhang, Y. S. Zhu, X. C. Wang, S. Dahl and I. Chorkendorff, *Angew. Chem., Int. Ed.*, 2013, **52**, 3621; J. Chen, S. Shen, P. Guo, P. Wu and L. Guo, *J. Mater. Chem. A*, 2014, **2**, 4605.
- 14 M. Miyauchi, M. Shibuya, Z. G. Zhao and Z. Liu, *J. Phys. Chem. C*, 2009, **113**, 10642.
- 15 M. Miyauchi, *Phys. Chem. Chem. Phys.*, 2008, **10**, 6258.
- 16 T. Arai, M. Horiguchi, M. Yanagida, T. Gunji, H. Sugihara and K. Sayama, *Chem. Commun.*, 2008, 5565; Q. Xiang, G. F. Meng, H. B. Zhao, Y. Zhang, H. Li, W. J. Ma and J. Q. Xu, *J. Phys. Chem. C*, 2010, **114**, 2049.
- 17 D. Bi and Y. Xu, *Langmuir*, 2011, **27**, 9359; H. Widiyandari, A. Purwanto, R. Balgis, T. Ogi and K. Okuyama, *Chem. Eng. J.*, 2012, **180**, 323.
- 18 H. Katsumata, Y. Oda, S. Kaneco and T. Suzuki, *RSC Adv.*, 2013, **3**, 5028.
- 19 L. Huang, H. Xu, Y. Li, H. Li, X. Cheng, J. Xia, Y. Xu and G. Cai, *Dalton Trans.*, 2013, **42**, 8606; Y. Zang, L. Li, Y. Zuo, H. Lin, G. Li and X. Guan, *RSC Adv.*, 2013, **3**, 13646; K. Katsumata, R. Motoyoshi, N. Matsushita, K. Okada, *J. Hazard. Mater.*, 2013, **260**, 475.
- 20 Z. Jin, N. Murakami, T. Tsubota, T. Ohno, *Appl. Catal. B*, 2014, **150/151**, 479; S. Chen, Y. Hu, S. Meng and X. Fu, *Appl. Catal. B*, 2014, **150/151**, 564.
- 21 Y. Zhang, J. Liu, G. Wu and Wei Chen, *Nanoscale*, 2012, **4**, 5300.
- 22 S.C. Yan, S.B. Lv, Z.S. Li and Z.G. Zou, *Dalton Trans.*, 2010, **39**, 1488.
- 23 K. Lee, W. S. Seo and J. T. Park, *J. Am. Chem. Soc.*, 2003, **125**, 3408.